JTTEE5 17:352–359
DOI: 10.1007/s11666-008-9180-6
1059-9630/$19.00 © ASM International

Preparation of Aluminum Coatings Containing Homogenous Nanocrystalline Microstructures Using the Cold Spray Process

A. C. Hall, L. N. Brewer, and T. J. Roemer

(Submitted October 1, 2007; in revised form April 9, 2008)

Nanostructured materials are of widespread interest because of the unique properties they offer. Well-proven techniques, such as ball milling, exist for preparing powders with nanocrystalline microstructures. Nevertheless, consolidation of nanocrystalline powders is challenging and presents an obstacle to the use of nanocrystalline metals. This work demonstrates that nanocrystalline aluminum powders can be consolidated using the cold spray process. Furthermore, transmission electron microscopy (TEM) analysis of the nanocrystalline cold spray coatings reveals that the cold spray process can cause significant grain refinement. Inert gas atomized 6061 and 5083 aluminum powders were ball milled in liquid nitrogen resulting in micron-sized powder containing 250-400 nm grains. Cold spray coatings prepared using these feed stock materials exhibited homogenous microstructures with grain sizes of 30-50 nm. TEM images of the as-received powders, ball-milled powders, and cold spray coatings are shown.

Keywords cold gas dynamic spraying of nanopowders, nanopowders, nanostructured coatings, nanostructured materials

1. Introduction

Nanostructured materials are of widespread interest to the scientific community because of the unique and unusual properties offered by these materials (Ref 1, 2). The high grain boundary content of nanocrystalline materials results in grain boundary properties contributing significantly to the bulk material properties. Dislocation behavior in nanocrystals is different from larger crystals and can result in significant strengthening of nanocrystalline metals (Ref 3, 4).

Many techniques have been developed for preparing nanocrystals including inert gas condensation, precipitation from solution, ball milling, rapid solidification, and crystallization from amorphous phases (Ref 1, 2). Many of these techniques result in free nanocrystals (precipitation and inert gas condensation) or in micron-sized powders (ball milling) containing nanocrystalline microstructures. One of the most challenging problems associated with nanocrystalline materials is the consolidation of these small powders into larger shapes that can be used for practical applications (Ref 2). This is a problem that Sandia National Laboratories is particularly interested in because of Sandia's interest in the manufacture of meso-scale machinery. Meso-scale machines are miniature mechanical systems. Individual components in these systems may have part dimensions on the order of a few hundred microns. The gears pictured in Fig. 1 were manufactured using traditional meso-scale machining (Ref 5-7) approaches not LIGA (Ref 8, 9) or MEMS techniques (Ref 10).

A number of problems are encountered in mesoscale parts as part dimensions approach the grain size of the base material including unpredictable mechanical behavior and reduced component performance. These problems stem from the fact that as component dimensions approach the grain size of the base material, grain boundary properties, and the orientation of individual grains dominate the mechanical behavior of the component. This problem can be solved by reducing the grain size in the base material.

One approach to preparing bulk material with nanocrystalline microstructures for the machining of meso-scale parts is to use the cold spray process to consolidate a feedstock powder containing a nanocrystalline microstructure. Preparation of micron size powder containing a nanocrystalline microstructure by ball milling under liquid nitrogen (LN_2) is well known (Ref 11, 2). Ajdelsztajn has shown previously that cold spray can be used to successfully consolidate LN_2 ball-milled powders containing a nanocrystalline microstructure (10-30 nm grain size) (Ref 12).

The goal of the work reported here is to demonstrate that cold spray is a feasible approach for preparing bulk metal shapes containing homogenous nanocrystalline

A. C. Hall and **L. N. Brewer**, Sandia National Laboratories, Albuquerque, NM; and **T. J. Roemer**, Ktech Corporation, Albuquerque, NM. Contact e-mail: achall@sandia.gov.

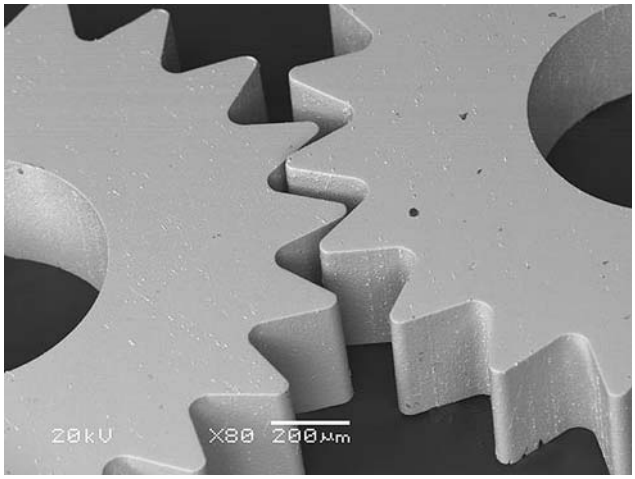

Fig. 1 Example of a meso-scale mechanical component. Fabrication of meso-scale mechanical components requires extremely fine-grained materials; otherwise component performance is determined by grain boundary locations and crystal orientations within the part

microstructures suitable for fabrication of meso-scale mechanical components. Once prepared, the intent is that cold-sprayed bulk metal shapes will be used as stock for machining meso-scale mechanical components. Near-net-shape forming followed by finish machining is not a goal of this work. Instead the intent is to prepare larger pieces of metal stock with grain sizes appropriate for meso-scale parts. The expectation is to machine multiple meso-scale components from a single cold spray nanocrystalline coating. This work only reports the feasibility of preparing metal stock with suitable microstructure, it does not address mechanical properties, aging, or machineability.

Cold spray is a well-known coating process in which a metal feedstock powder is sprayed at high velocity (~1000 m/s) and low temperature (<100 °C) (Ref 13). A cold spray torch consists of a converging-diverging nozzle, a gas control system, a powder feed system, and a gas heater. Feedstock powder is injected into a high pressure (>200 psig) He or N_2 gas flow just upstream of a converging-diverging nozzle. The powder is entrained in the gas stream and reaches supersonic velocities as it travels through the nozzle. The propulsion gas stream is often heated to moderate temperatures (<600 °C) to increase the sonic velocity of the gas and thus increase the particle velocity. Heating of the propulsion gas typically does not result in significant powder heating (Ref 14). Upon impact with the substrate, the metal powder experiences significant mechanical deformation. This deformation causes a hydrodynamic instability to form at the particle-substrate contact allowing breakup of surface oxides, shear along the particle-substrate interface, and ejection of material from the particle-substrate interface. This process results in mechanical and metallurgical bonding between the particle and substrate. It also results in significant plastic deformation of the impacting particle as well as the substrate in the immediate vicinity of the impacting particle. As subsequent particles impact and consolidate a coating or bulk shape is formed (Ref 15, 16). Process vectors for cold spray are well understood. As particle velocity increases deposition efficiency, coating density, residual stress, and coating adhesion strength all increase (Ref 14).

The mechanisms responsible for nanocrystal formation during the ball milling process are also well understood. Fecht (Ref 11) explains that nanocrystals form during severe plastic deformation in three stages. Initially high-density arrays of dislocations are formed. As plastic deformation continues these dislocations annihilate and recombine forming subgrains with low angle grain boundaries. Further deformation causes the subgrains to rotate forming high angle grain boundaries.

2. Experimental Procedures

2.1 Feedstock

The 5083 aluminum powder was purchased from Novomac LLC, (Dixon, CA, USA). The 6061 aluminum powder was purchased from Valimet (Stockton, CA, USA). Both powders were produced using inert gas atomization. All LN_2 ball milling of these powders was conducted by Novomac LLC using a proprietary, high efficiency, LN_2 ball-milling process. All powder size distribution measurements were made using a Beckman-Coulter Laser Diffraction Particle Size Analyzer. This machine is a dry-type particle size analyzer using a Fraunhaufer diffraction criterion to determine particle size distribution. A field emission SEM was used to determine the morphology of each powder.

2.2 TEM Sample Preparation and Imaging

Transmission electron microscopy (TEM) samples were prepared using the focused ion beam (FIB) lift-out technique. This procedure used a dual electron-Ga ion beam instrument (FEI DB-235). For the starting powders, particles were sprinkled onto carbon tape on an aluminum stub. Areas on the surface of a given particle were selected and coated with electron beam and ion beam deposited platinum to protect the surface of the section during ion milling. TEM sections approximately 10 μm by 5 μm by 200 nm were milled using a 30 keV Ga ion beam. The section was then ion polished with a 5 keV Ga ion beam prior to detachment and lift-out. The resultant TEM section was placed onto a thin carbon membrane on a copper TEM grid. For the sprayed coatings, the process was identical except that the sample was simply placed into the chamber in a plan view orientation, and an area for analysis was chosen.

The TEM characterization was performed using a Phillips CM30 TEM at 300 keV. Bright field images, dark field images, and diffraction patterns were collected using both a solid-state image plate system (DITABIS) and a Gatan Image Filter (GIF) camera.

2.3 Cold Spray

Cold spraying was conducted at Sandia's Thermal Spray Research Laboratory in Albuquerque, NM using a cold spray system that was designed and built by Ktech Corp. Albuquerque, NM. The cold spray nozzle used for these experiments had a 2.0-mm diameter throat, a 100-mm long supersonic region, and a 5-mm diameter exit orifice. Helium was used as the propulsion gas. All coatings were sprayed a using 2410 kPa (350 psig), 350 °C He flow. All samples were prepared using a raster speed of 50 mm/s, a raster step size of 1 mm, and a standoff distance of 25 mm. All coatings were prepared on 6061 aluminum substrates that were grit blasted and solvent cleaned prior to spraying.

3. Results

3.1 Powder, Morphology, Microstructure, and Size Distribution

Powder size distributions for the as-received 5083 and 6061 powders are shown in Fig. 2. Figure 3 shows the powder size distributions for the LN_2 ball-milled 5083 and 6061 powders. All of the powders have Gaussian powder size distributions. Table 1 shows the mean particle sizes and approximate mean particle velocities at the spray conditions used to prepare the coatings reported here. All particle velocities in Table 1 were calculated using the method described by Dykhuizen and Smith (Ref 17), Eq #20. The measured mean size of both the 6061 and 5083 powders increased as a result of ball milling. SEM images of the as-received powder and the LN_2 ball-milled powder Fig. 4 and 5, respectively, show that these powders were flattened considerably during the ball-milling process and are now flake-like, as expected. It is likely that the

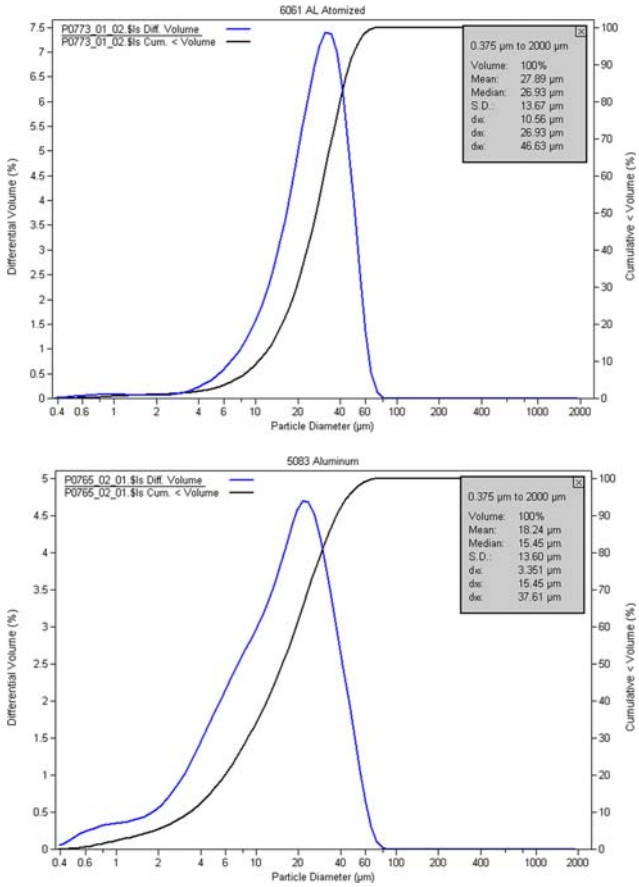

Fig. 2 Powder size distribution measurements for the as-received 6061 atomized (*top*), and the 5083 atomized (*bottom*) feed stocks

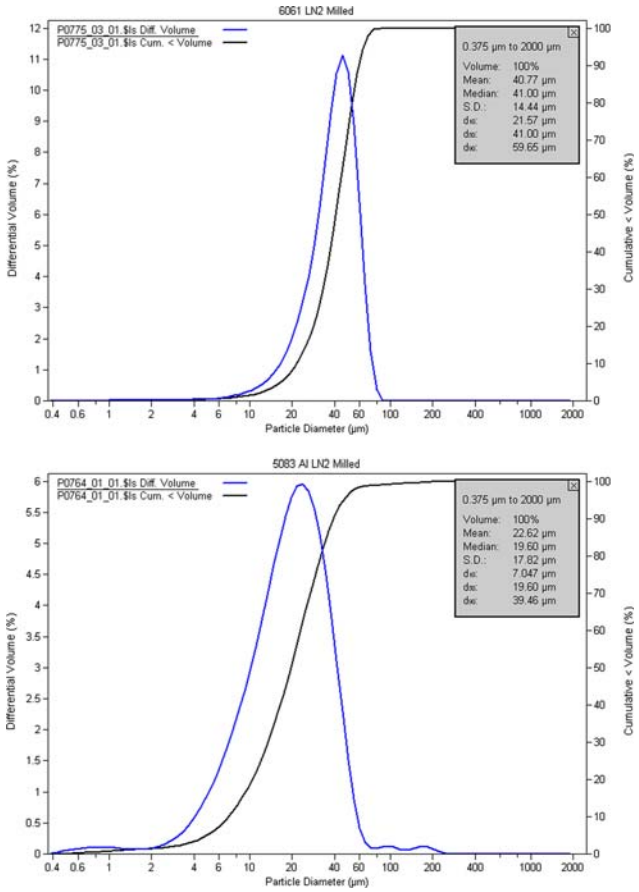

Fig. 3 Powder size distributions for the 6061 (*top*) and 5083 (*bottom*) powders after LN2 ball milling

Table 1 Mean particle sizes and corresponding particle velocities achieved with a 2410 kPa (350 psig), 350 °C He flow

Powder	Mean size, µm	Calculated mean centerline particle velocity, m/s
6061 as-received	27.8	1137
5083 as-received	18.2	1264
6061 LN2 ball milled	40.7	1022
5083 LN2 ball milled	22.6	1199

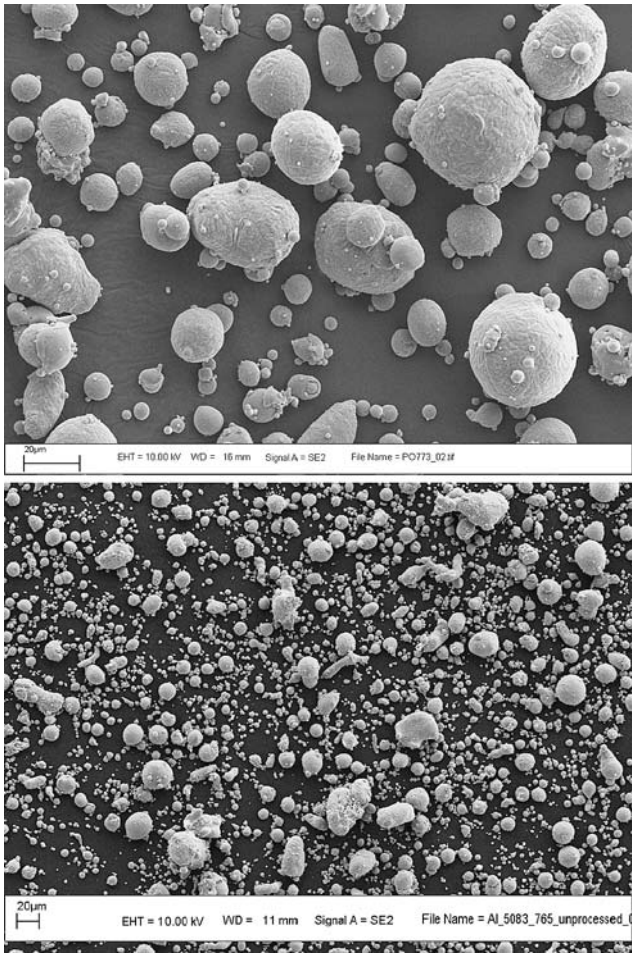

Fig. 4 SEM images showing the as-received morphology of the atomized 6061 (*top*), and the atomized 5083 (*bottom*) powders

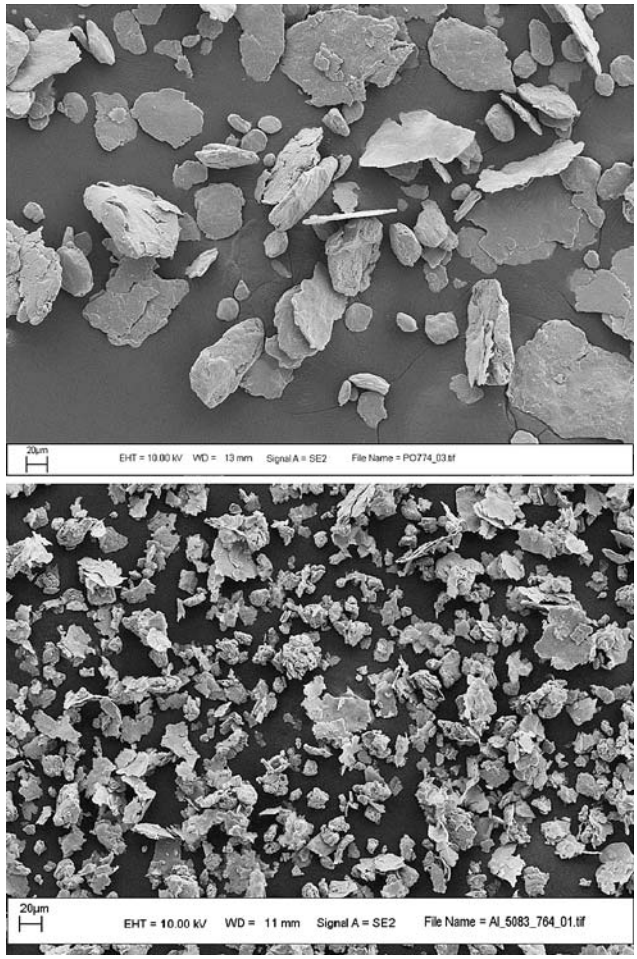

Fig. 5 SEM images showing the morphology of the LN2 ball milled 6061 (*top*), and the LN2 ball milled 5083 (*bottom*) powders

powder size measurement was skewed by the high aspect ratio of the ball-milled particles. The Beckman-Coulter instrument assumes a spherical particle.

The ball-milling process causes considerable flattening of the powder. This makes the powder more difficult to feed into the cold spray process, use of a pneumatic vibrator on the hopper is necessary, but does not appear to otherwise affect its behavior.

Figure 6 shows TEM images of coatings prepared using the as-received 6061 and 5083 powders. Grain sizes in both of these coatings are on the order of microns. Figure 7 shows TEM images of the LN_2 ball-milled powders. The LN_2 ball-milled 6061 powder has an ultra-fine grained structure. The LN_2 ball-milled 5083 powder has an elongated nano-crystalline structure. After LN_2 ball milling, the 6061 grain size is between 250 and 400 nm. The 5083 grains are 20-40 nm in width but are highly elongated. Distinct morphological texture was observed for both ball-milled powders. The microstructure consisted of elongated lamellar or pancake-shaped grains with lengths 5-15 times their thickness. These grains were also oriented parallel to the surface of the powder particle and are likely the result of deformation associated with the ball-milling process. Despite the strong morphological texture in the LN_2 ball-milled powders, there was no particularly significant crystallographic texture observed in the selected area diffraction patterns (Fig. 7). Note: All of the grain sizes given in this paper were determined using the TEM images shown. Thus, grain sizes are given as a range (e.g., 20-40 nm) and are somewhat approximate.

3.2 Coating Microstructures

Nanocrystalline 5083 and 6061 coatings were prepared on 50.8 mm × 50.8 mm × 3.175 mm (2″ × 2″ × 1/8″) aluminum substrates. Figure 8 is a picture of the two coated test coupons. The 5083 coating is 0.058 mm (0.0023″) thick. The 6061 coating is 0.513 mm (0.0202″) thick.

Figures 9 and 10 are TEM images showing microstructures of coatings prepared using the as-received and LN_2 ball-milled powders. All coatings prepared with the as-received powders exhibited micron-sized grains, as expected. However, both coatings prepared using the LN_2 ball-milled powders exhibited 30-50 nm grain sizes. This was unexpected given the elongated grains in both

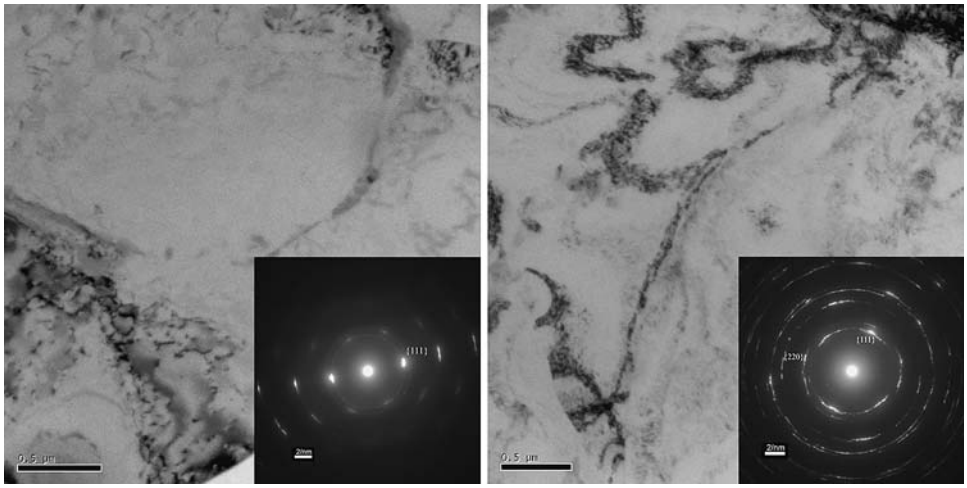

Fig. 6 TEM images of coating prepared using the as-received atomized 6061 (*left*) and as-received atomized 5083 (*right*) powders. Grain sizes are large (>1 μm for 6061 (*left*), >500 nm for 5083 (*right*)). SADP from 6061 (*left*) is from a single grain, SADP from 5083 (*right*) shows heavily smeared spots from deformed grains. Scale bars are 0.5 μm

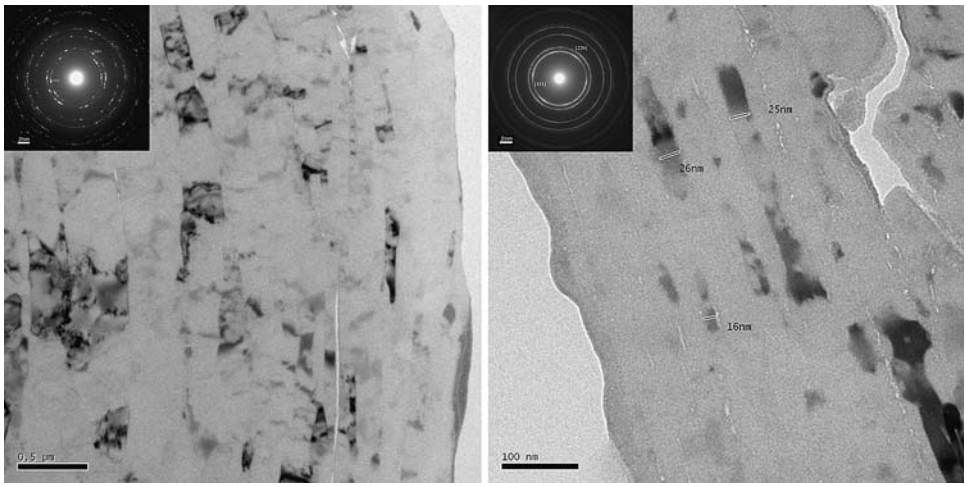

Fig. 7 TEM images showing the microstructure of the 6061 (*left*) and 5083 (*right*) powders after LN2 ball milling. Notice that both powders have elongated grains. The grains in the 6061 have refined to ~250-400 nm. The grains in the 5083 have nanometer scale widths, but are highly elongated. Both selected area diffraction patterns show that the ball-milled materials have no texture. Scale bars are 0.5 μm

powders and the 250-400 nm grain size in the 6061 LN_2 ball-milled powder. In both cases, no crystallographic texture was observed in the diffraction patterns from the coatings. Additionally, a good deal of nano-scale porosity was observed in these coatings. The porosity was highly aligned with lath boundaries in the 5083 alloy with much less alignment in the 6061 alloy.

4. Discussion

4.1 Grain Refinement

As shown by the TEM images above (Fig. 6, 7, 9, and 10), the cold spray process resulted in significant grain refinement for both the 6061 and the 5083 LN_2 ball-milled powders. The grain size reduction from 250 to 400 nm in the LN_2 ball-milled 6061 powder to 30-50 nm in the cold-sprayed coatings is approximately a factor of eight in grain size and close to a factor of 70 in grain volume. The grain refinement in the 5083 is similarly dramatic. The elongated 5083 grains are equiaxed in the cold-sprayed coating. Most likely this grain refinement occurred through mechanisms similar to those proposed by Fecth (Ref 11). It is reasonable to expect that the deformation associated with the cold spray process could result in sufficient dislocation generation and subgrain rotation to cause grain refinement. Grain refinement during the cold spray process has been documented before in pure aluminum of normal grain size (Ref 16). The lath structure in the LN_2 ball-milled powder appears to be retained in the 5083 cold spray coating.

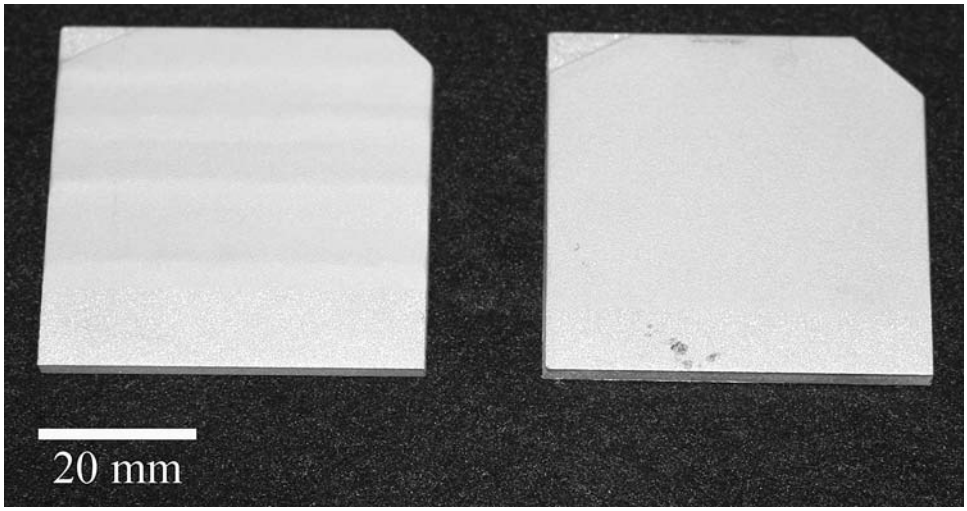

Fig. 8 As sprayed nanocrystalline aluminum coatings: 5083 (*right*) and 6601 (*left*)coupons are shown

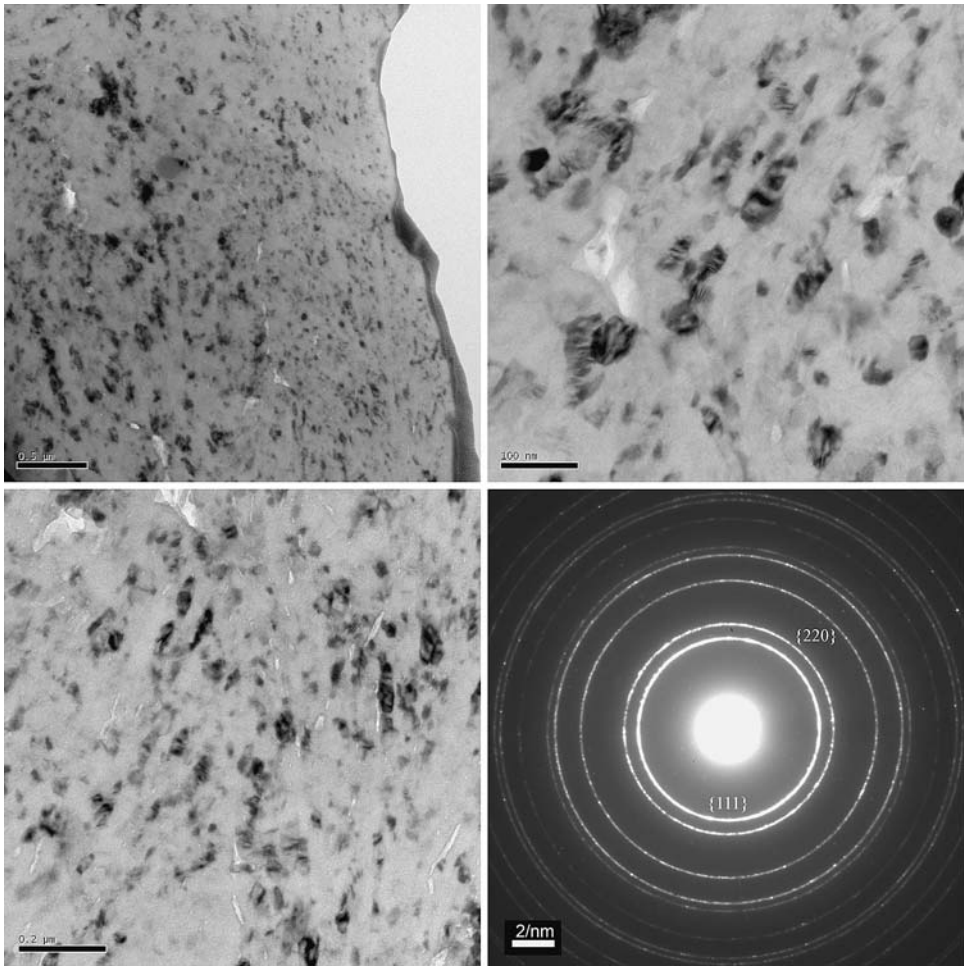

Fig. 9 Three TEM images showing the microstructure of the cold spray coating prepared using the LN2 ball milled 6061 powder. The selected area diffraction pattern (SADP) shows complete rings with no discernable texture. Scale bars are 0.5 μm (*top right*), 0.2 μm (*bottom right*), and 100 nm (*top left*)

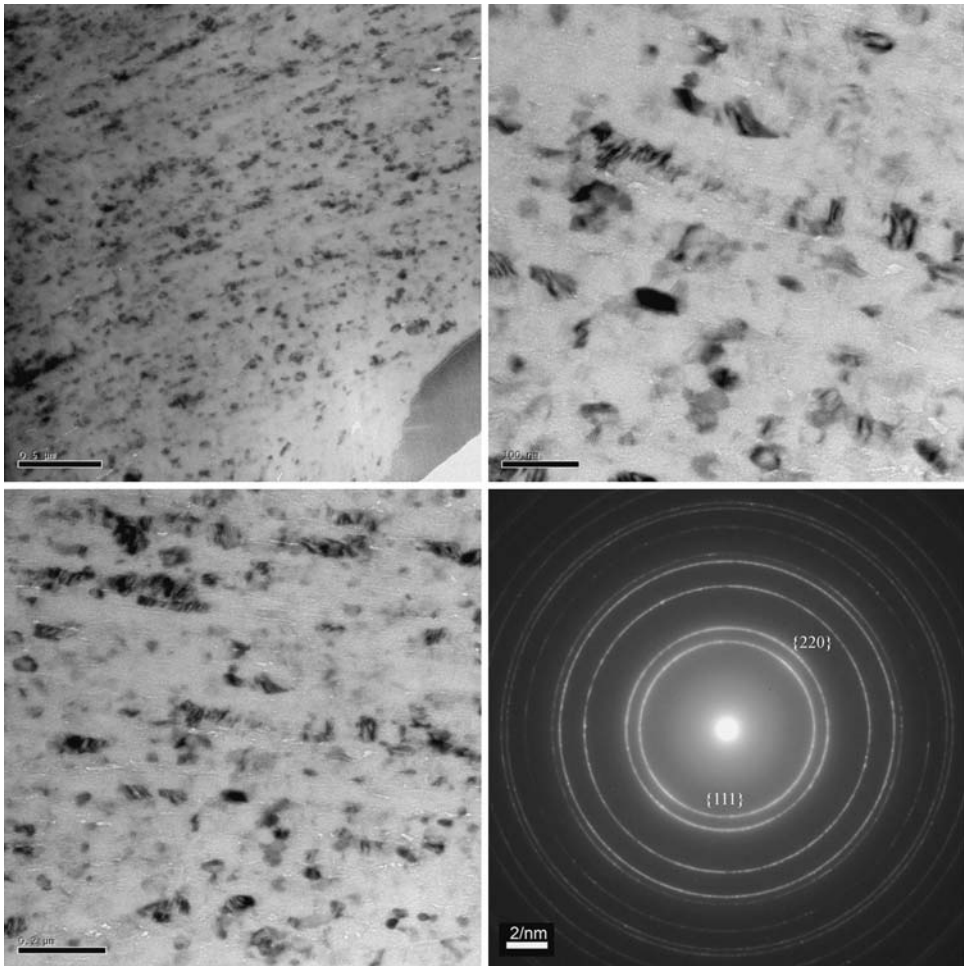

Fig. 10 Three TEM images showing the microstructure of the cold spray coating prepared using the LN2 ball milled 5083 powder. The SADP shows complete rings with no discernable texture. Scale bars are 0.5 μm (*top right*), 0.2 μm (*bottom right*), and 100 nm (*top left*)

Interestingly, the observation of grain refinement as a result of the cold spray process reported here appears to be in direct contrast to the results reported by Ajdelsztajn (Ref 11) in 2005. Ajdelsztajn also used the cold spray process to consolidate LN_2 ball-milled 5083 aluminum powder. This study clearly showed that the cold spray process is an effective method of consolidating nanocrystalline powders. However, Ajdelsztajn reported that no grain refinement was observed during the cold spray process. The nanocrystalline grains in Ajdelsztajn's coating were of similar size to the nanocrystalline grains in the LN_2 ball-milled 5083 Al powder sprayed at Sandia. While the results of these two studies may appear to be in contrast; they are not. The experiment reported here was substantially different from Ajdelsztajn's experiment in two important ways. First, Ajdelsztajn's spray conditions were significantly different from the conditions used in this experiment. This may have resulted in lower average particle velocity in Ajdelsztajn's experiment. Ajdelsztajn's experiment used a room temperature 1.7 MPa (~250 psig) helium flow to propel the particles. The experiments reported here used a 2410 kPa (350 °C), 350 psig Helium flow to propel the particles. Thus, more energy and more plastic deformation were available in this experiment compared to Ajdelsztajn's experiment. Second, and more importantly, Ajdelsztajn's 5083 aluminum feedstock was ball milled to a grain size of 20-30 nm before spraying. Work by Romanov and Eckert suggests that it may become increasingly difficult or impossible to create grain sizes in aluminum smaller than 20 nm by plastic deformation mechanisms (Ref 3, 17). Romanov explains that a critical crystal size exists below which gliding dislocations are unstable due to image forces. In aluminum Romanov estimates the critical size for dislocation stability as 18 nm. Below this size, gliding dislocations will be unstable and will rapidly move to grain boundaries or annihilate. Instability of dislocations would make it more difficult to create the dislocation networks, subgrain boundaries, and ultimately the high angle grain boundaries required for deformation-induced grain refinement. Eckert (Ref 17) explicitly considers the problem of minimum grain size obtainable by ball milling and explains that minimum grain size is determined by a competition between plastic deformation and the recovery behavior of the material.

Minimum grain size for aluminum is shown to be between 20 and 25 nm.

5. Conclusions

This experiment clearly demonstrates that cold spray can be used to refine the microstructure of an ultra-fine-grained (100's of nm grain size) powder and consolidate it to create a homogenous nanocrystalline (20-40 nm) microstructure. When compared to the work of Ajdelsztajn which shows that the cold spray process can be used to consolidate nanocrystalline aluminum without causing recrystallization it illustrates the flexibility of the cold spray process. This flexibility is typical of spray processes and highlights the need to further understand the process-microstructure-property relationships in nanocrystalline cold spray coatings. The cold spray process is likely an extremely controllable method for preparing metal coatings and bulk metal shapes with homogenous nanocrystalline microstructures. If grain refinement in the cold spray process is occurring by the mechanism proposed by Fecth (Ref 11), cold spray should be capable of preparing nanocrystalline microstructures from almost any sprayable metal feedstock. The following specific conclusions were reached from the data presented in this study:

1. The cold spray process can cause the refinement of ultra fine-grained powdered aluminum feed stocks creating a homogenous nanocrystalline microstructure.
2. Grain refinement observed in Al due to cold spray occurs because of the severe plastic deformation associated with the cold spray process.

Acknowledgments

The authors would like to acknowledge Dr. Leonardo Ajdelsztajn for his advice on sources for LN_2 ball-milled powder and for his insightful work on cold-sprayed nanocrystalline aluminum. It was a foundation and significant motivator for the experiments reported here.

References

1. H. Gleiter, Nanostructured Materials: State of the Art, *Perspect. NanoStruct. Mater.*, 1995, **6**(1-4), p 3-14
2. C.C. Koch, Synthesis of nanostructured Materials By Mechanical Milling: Problemens and Opportunities, *NanoStruct. Mater.*, 1997, **9**(1), p 13-22
3. A.E. Romanov, Continuum Theory of Defects in Nanoscaled Materials, *NanoStruct. Mater.*, 1995, **6**(1-4), p 125-134
4. J.R. Trelewicz and C.A. Schuh, The Hall-Petch Breakdown in Nanocrystalline Metals: A Crossover to Glass-Like Deformation, *Acta Mater.*, 2007, **55**, p 5948-5958
5. A.B. Frazier, R.O. Warrington, and C. Friedrich, The Miniaturization Technologies: Past; Present; and Future, *IEEE Trans. Industr. Electr.*, 1995, **42**(5), p 423-430
6. K.N. Bhat, Micromachining for Microelectromechanical Systems, *Defense Sci. J.*, 1998, **48**(1), p 5-19
7. D.P. Adams, M.J. Vasile, and A.S.M. Krishnan, Microgrooving and Microthreading Tools for Fabricating Curvilinear Features, *Precision Eng. J. Intl. Soc. Precision Eng. Nanotechnol.*, 2000, **24**(4), p 347-356
8. J. Mohr, LIGA: A Technology for Fabricating Microstructures and Microsystems, *Sensors Mater.*, 1998, **10**(6), p 363-373
9. W. Bacher, W. Menz, and J. Mohr, The LIGA Technique and Its Potential for Microsystems—A Survey, *IEEE Trans. Industr. Electr.*, 1995, **42**(5), p 431-441
10. S.M. Spearing, Materials Issues in Microelectromechanical Systems, *Acta Mater.*, 2000, **48**, p 179-196
11. H.J. Fecht, Nanostructure Formation by Mechanical Attrition, *NanoStruct. Mater.*, 1995, **6**(1-4), p 33-42
12. L. Ajdelsztajn, B. Jodoin, G.E. Kim, J.M. Schoenung, and J. Mondoux, Cold Spray Deposition of Nanocrystalline Aluminum Alloys, *Metall. Mater. Trans. A*, 2005, **36A**, p 657-666
13. P. Alkimov, V.F. Kosarev, and A.N. Papyrin, A Method of Cold Gas-Dynamic Deposition, *Sov. Phys. Dokl.*, 1990, **35**(12), p 1047-1049
14. D.L. Gilmore, R.C. Dykhuizen, R.A. Neiser, T.J. Roemer, and M.F. Smith, Particle Velocity and Deposition Efficiency in the Cold Spray Process, *J. Thermal Spray Technol.*, 1999, **8**(4), p 576-582
15. R.C. Dykhuizen, M.F. Smith, D.L. Gilmore, R.A. Neiser, X. Jiang, and S. Sampath, Impact of High Velocity Cold Spray Particles, *J. Thermal Spray Technol.*, 1999, **8**(4), p 559-564
16. A.C. Hall, D.J. Cook, R.A. Neiser, T.J. Roemer, and D.A. Hirschfeld, The Effect of a Simple Annealing Heat Treatment on the Mechanical Properties of Cold-Sprayed Aluminum, *J. Thermal Spray Technol.*, 2006, **15**(2), p 233-238
17. R.C. Dykhuizen and M.F. Smith, Gas Dynamic Principles of Cold Spray, *J. Thermal Spray Technol.*, 1998, **7**(2), p 205-212
18. J. Eckert, Relationships Governing the Grain Size of Nanocrystalline Metals and Alloys, *NanoStruct. Mater.*, 1995, **6**(1-4), p 431-416